Corticogeniculate feedback sharpens the temporal precision and spatial resolution of visual signals in the ferret

J. Michael Hasse[a,b] and Farran Briggs[a,b,1]

[a]Department of Physiology & Neurobiology, Geisel School of Medicine, Dartmouth College, Lebanon, NH 03756; and [b]Program in Experimental and Molecular Medicine, Dartmouth College, Hanover, NH 03755

The corticogeniculate (CG) pathway connects the visual cortex with the visual thalamus (LGN) in the feedback direction and enables the cortex to directly influence its own input. Despite numerous investigations, the role of this feedback circuit in visual perception remained elusive. To probe the function of CG feedback in a causal manner, we selectively and reversibly manipulated the activity of CG neurons in anesthetized ferrets in vivo using a combined viral-infection and optogenetics approach to drive expression of channelrhodopsin2 (ChR2) in CG neurons. We observed significant increases in temporal precision and spatial resolution of LGN neuronal responses to drifting grating and white noise stimuli when CG neurons expressing ChR2 were light activated. Enhancing CG feedback reduced visually evoked response latencies, increased spike-timing precision, and reduced classical receptive field size. Increased precision among LGN neurons led to increased spike-timing precision among granular layer V1 neurons as well. Together, our findings suggest that the function of CG feedback is to control the timing and precision of thalamic responses to incoming visual signals.

corticothalamic | LGN | V1 | feedback | optogenetics

The feedforward progression of sensory information from peripheral receptors through nuclei in the sensory thalamus to the primary sensory cortex is well understood. For example, much is known about how neurons in the primary sensory cortex represent elementary sensory features based on the inputs they receive from peripheral and thalamic neurons with well-defined receptive field properties. In addition to these feedforward circuits, mammalian sensory systems include a substantial feedback projection from the primary sensory cortex to the sensory thalamus (1). Despite a rich history of investigation, the functional role of corticothalamic feedback circuits in sensory perception remains a fundamental mystery in neuroscience.

Our goal was to determine the functional contribution of corticothalamic feedback to vision. Corticogeniculate (CG) circuits link the primary visual cortex (V1) with the lateral geniculate nucleus of the thalamus (LGN) and constitute the first cortical feedback connection in the visual processing hierarchy (2). CG axons target LGN relay neurons, local interneurons within the LGN, and neurons in the visual portion of the thalamic reticular nucleus (TRN) that inhibit LGN relay neurons (3–5) (Fig. 1A). Based on this pattern of axonal innervation, CG modulation of LGN neurons could include both monosynaptic excitation and disynaptic inhibition of LGN relay neurons via TRN and/or local LGN inhibitory circuitry. The CG circuit is anatomically robust—cortical synapses onto LGN relay neurons far outnumber retinal synapses (4); however, the receptive fields of LGN relay neurons reflect their retinal and not their cortical inputs (6). In part due to its subtle influence on LGN responses, the function of CG feedback has remained elusive.

There have been numerous experimental examinations of CG function—using methods with varying degrees of selectivity and/or reversibility of CG manipulation—and a corresponding variety of proposed functional roles for feedback. Some have proposed that

CG feedback modulates the gain (7–14) and/or the spatiotemporal properties of LGN neurons (15–17). Others have proposed that corticothalamic feedback controls whether thalamic neurons are in a state of net excitation or inhibition (8, 12), depending upon oscillatory activity in corticothalamic networks (18). Our goal was to conduct a causal and comprehensive examination of CG function using a combination of virus-mediated gene delivery and optogenetic strategies to selectively and reversibly manipulate the activity of CG neurons in vivo. We examined CG function in the ferret, a visual carnivore and useful model of visual system development and function (19). We systematically measured visual responses of ferret LGN neurons to a variety of stimuli while CG feedback was optogenetically enhanced. We discovered that enhancing CG feedback significantly reduced visual response latencies, increased spike-timing precision, and increased spatial resolution among LGN neurons. Enhancing CG feedback did not alter contrast sensitivity or spatial/temporal frequency tuning preferences of LGN neurons, although LGN neuronal responses to gratings varying in temporal frequency were slightly enhanced. Our findings suggest that the overall function of corticothalamic feedback in sensory perception is to control the temporal precision and spatial resolution of thalamic responses to incoming sensory inputs to boost the efficacy of feedforward signal transmission to the cortex.

Results

Using optogenetics, a technology that enables selective and reversible manipulation of neuronal activity in the intact brain (20), we performed a causal experiment to determine the influence of CG feedback on LGN neurons. To selectively and reversibly manipulate

Significance

The functional role of corticothalamic circuits, connecting the cortex to the thalamus in the feedback direction, has remained a fundamental mystery in neuroscience. In spite of the fact that corticothalamic inputs are numerous, their influence on thalamic activity is modest. We used an innovative combination of virus-mediated gene delivery and optogenetics to probe the function of corticothalamic feedback in vision. We found that corticothalamic feedback does not alter the visual response properties of thalamic neurons, but instead controls the timing and fidelity of their responses to incoming visual inputs. Thus, our results provide an answer to a long-standing question in neuroscience: A key function of corticothalamic feedback is to control the timing and precision of thalamic responses.
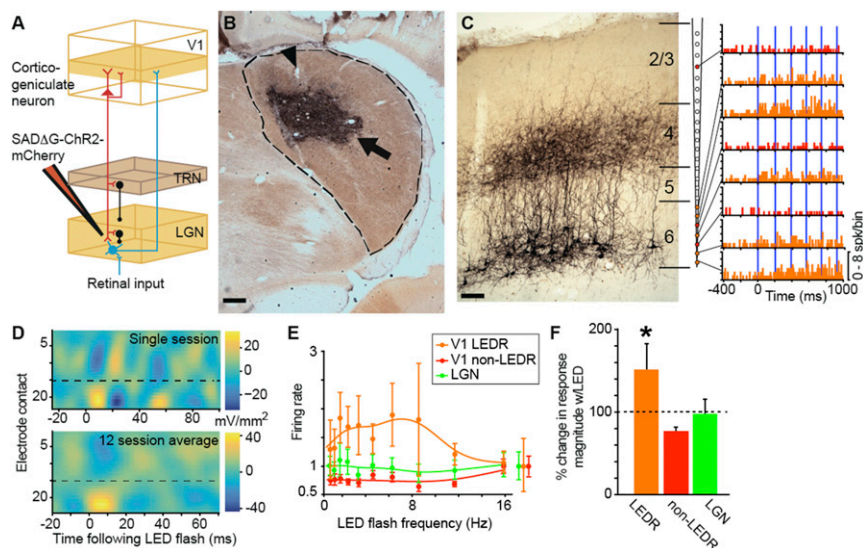
Fig. 1. Virus injection and LED stimulation of putative CG neurons. (*A*) Schematic representation of the CG feedback circuit and injection of SADΔG-ChR2-mCherry into the LGN, resulting in retrograde labeling of CG neurons (red). Feedforward projections (retinal axons and LGN relay neurons) are in cyan; inhibitory interneurons (from TRN and within the LGN) are in black. (*B*) Coronal section through the LGN (dashed line) illustrating the virus injection zone (arrow) and electrode lesions (arrowhead). Dorsal is up, medial is left. (Scale bar, 375 μm.) See *SI Appendix*, Fig. S1 *A and B* for additional examples. (*C*, *Left*) Coronal section through V1 (area 17) illustrating CG neurons expressing mCherry. (Scale bar, 250 μm.) Cortical layers are indicated by horizontal lines and labeled. (*C*, *Right*) Lines connect peristimulus-time histograms to recording contacts on the schematic linear array (orange and red PSTHs indicate LEDR and non-LEDR neurons, respectively). Blue lines indicate 5-ms LED flashes. Note that all LEDR neurons are located on deep contacts (orange-filled circles on the array). (*D*) Current-source density profiles of local field potential responses to LED-only stimulation for a single session (*Top*) and averaged across 12 sessions (*Bottom*). Low-number electrode contacts are closest to the pial surface; dashed lines indicate the border between layers 4 and 5. (*E*) Population LED tuning curves for 15 V1 LEDR neurons (orange), 19 V1 non-LEDR neurons (red; within 147 μm of LEDR neurons), and 21 LGN neurons (green). Normalized spontaneous activity levels for each neuron type are indicated to the right of the curves. Error bars represent SEMs. (*F*) Percent change in response magnitude relative to spontaneous activity levels (indicated by the dashed line) with LED-only stimulation for V1 LEDR neurons ($n = 15$; orange; average change in LEDR response magnitude is $152 \pm 31\%$), neighboring V1 non-LEDR neurons within 147 μm on average of LEDR neurons ($n = 19$; red; average change in non-LEDR response magnitude is $77 \pm 5\%$), and LGN neurons ($n = 21$; green; average change in LGN response magnitude is $98 \pm 17.3\%$). Error bars represent SEMs, and the asterisk indicates that the LED significantly enhanced the magnitude of V1 LEDR neuronal responses compared with other V1 and LGN neurons, which were not modulated ($P = 0.0002$). spk, spike; w/, with.

the activity of CG neurons in ferrets, we used a glycoprotein (G)-deleted rabies virus (SADΔG-ChR2-mCherry) that acts as a vehicle for the delivery and expression of optogenetic (channelrhodopsin2; ChR2) and fluorescent (mCherry) proteins (21, 22). G-deleted rabies virus is taken up by axon terminals and moves exclusively in the retrograde direction to infect cell bodies but is prohibited from crossing synapses (22–25). We took advantage of the fact that CG neurons are the only visual cortical neurons that project axons to the LGN (26–28), combined with the exclusively retrograde action of G-deleted rabies virus, to selectively infect CG neurons following injection of virus into the LGN (29) (Fig. 1*A*). In 11 adult ferrets, we injected small volumes (∼5 μL) of virus into the LGN (Fig. 1*B* and *SI Appendix*, Fig. S1 *A and B*), which resulted in virus infection of multiple neuronal populations including retinogeniculate neurons, TRN neurons, LGN interneurons (*SI Appendix, Results* and Figs. S1*B* and S2*A*), and CG neurons (Fig. 1*C* and *SI Appendix*, Fig. S1 *C and D*). Consistent with prior studies of retrograde-labeled CG neurons (26, 29–31), virus-infected CG neurons were entirely restricted to layer 6 of areas 17 and 18 in the visual cortex (Fig. 1*C* and *SI Appendix*, Fig. S1 *C and D*). In 9 control animals, virus injections into structures surrounding the LGN, including the white matter, ventricle, hippocampus, and somatosensory cortex, resulted in no infected neurons in the LGN or visual cortex, indicating that virus was not taken up by axons of passage.

Seven to 11 days following surgical injection of virus into the LGN, we performed neurophysiological recordings of V1 and LGN neurons while animals were anesthetized and paralyzed. We inserted a 24-contact linear multielectrode array into V1 and verified post hoc that electrodes were placed within patches of infected CG neurons (*SI Appendix*, Fig. S1*D*). We also placed a

7-channel multielectrode array into the LGN such that V1 and LGN recording sites were retinotopically aligned (*SI Appendix*, Figs. S1*A* and S2*F*). To verify that infected CG neurons were directly modulated by LED stimulation, we recorded extracellularly from neurons spanning the full cortical depth of V1 in four experimental animals, and measured neuronal responses to LED flashes focused on the V1 cortical surface in the absence of visual stimulation. LED flashes in the absence of visual stimulation directly modulated spiking activity of individual V1 neurons located on deep-layer contacts of the linear array (Fig. 1*C*) and modulated population activity within V1, beginning with a current sink localized to layer 6 that was time-locked to LED flash onset (Fig. 1*D*). Putative CG neurons, termed LED-responsive (LEDR) neurons, were defined according to three criteria: location on deep-layer contacts of the linear array, time-locked LED-only stimulation of local field potentials recorded from the same contacts, and significant LED-only modulation of firing rate (Fig. 1 *E* and *F*; see *SI Appendix, Materials and Methods* for further details). Our "hit rate" for recording LEDR neurons was 75%. The average LED flash onset response latency among LEDR neurons was 5.7 ± 1.2 ms (LED flashes were ∼5 ms in duration), indicating that individual LEDR neuronal responses to LED flashes were fast and time-locked, with little temporal jitter (see *SI Appendix, Results* for further details). LED flashes at increasing flash frequencies significantly enhanced the response magnitude of LEDR neurons ($P = 0.0002$) but did not change the responses of other V1 neurons (non-LEDR neurons) or LGN neurons relative to spontaneous levels (Fig. 1 *E* and *F*). Only 2 out of 21 LGN neurons demonstrated a significant increase in response magnitude with LED-only stimulation, likely due to high convergence of infected CG axons onto these neurons
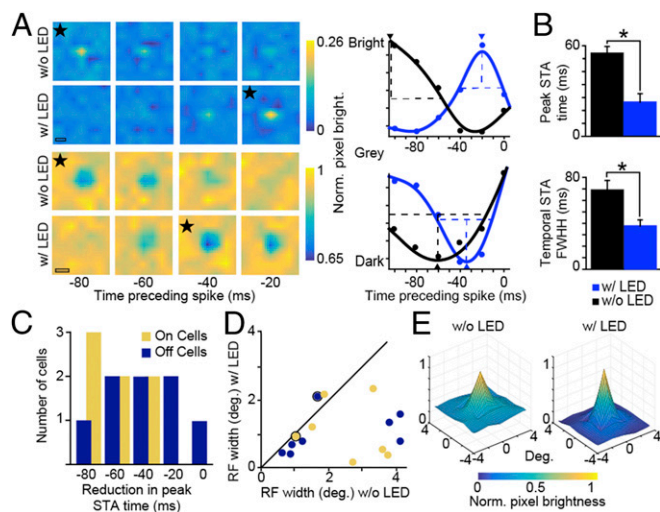
Fig. 2. LED stimulation of CG feedback reduces spatiotemporal response latency and full width at half height. (*A*, *Left*) Spike-triggered averages for representative LGN ON (*Top* two rows) and OFF (*Bottom* two rows) neurons with and without LED stimulation. Stars identify frames with peak pixel brightness; the interior height of the scale bars illustrates the width of each pixel in the grid; and the color bars illustrate pixel brightness values. (Scale bars, 2.5°.) (*A*, *Right*) Temporal STA curves (Gaussian fits to data, indicated by dots) for the same neurons without (black) and with (blue) LED stimulation. Arrowheads show temporal STA peaks; dashed lines show full width at half height (FWHH; cutoff for without LED response). (*B*) Average peak STA time (absolute values used) and FWHH of temporal STA without (black) and with (blue) LED stimulation for 15 LGN neurons. Error bars represent SEMs; asterisks indicate statistically significant differences at $P \le 0.01$. (*C*) Histogram of reduction in peak STA time with LED stimulation for LGN ON (gold; $n = 7$) and OFF (dark blue; $n = 8$) neurons. (*D*) Comparisons of classical receptive field (RF) width (degrees) for ON (gold; $n = 7$) and OFF ($n = 8$ neurons from six experimental animals) LGN neurons with and without LED stimulation. Dots with black rings indicate the ON and OFF neurons illustrated in *A*. (*E*) Aggregate receptive fields for the 15 LGN neurons illustrated in *C* and *D* (OFF neuronal response polarities were flipped) without (*Left*) and with (*Right*) LED stimulation of CG feedback. *y* axes are normalized pixel brightness as indicated by the color bar beneath. Individual neuronal spatial receptive fields were scaled according to the without-LED response and averaged together to generate aggregate receptive fields. bright, brightness; deg, degrees; Norm, normalized; w/, with; w/o, without.

(*SI Appendix, Results* and Fig. S2). Importantly, the LED had no impact on LGN or V1 neuronal activity in control animals, in which no CG neurons expressed ChR2 (*SI Appendix, Results* and Fig. S2*E*). Furthermore, spontaneous and visually evoked firing rates of LGN and V1 neurons were not statistically different across experimental and control animals, indicating that virus infection did not alter neuronal physiology (*SI Appendix, Results*).

CG Feedback Reduces Response Latency and Increases Spike-Timing Precision Among LGN Neurons. Having verified that LED stimulation activated virus-infected CG neurons in vivo, we next examined neuronal responses to visual stimuli under conditions with and without LED stimulation of CG feedback. In six experimental animals, we measured neuronal responses to m-sequence stimuli with and without continuous LED illumination. Continuous LED illumination paired with m-sequence visual stimulation increased the magnitude of V1 LEDR neuronal responses but did not alter overall response patterns relative to m-sequence-only stimulation and did not cause long-term saturation or suppression of LEDR neuronal activity (*SI Appendix, Results* and Fig. S3). Fig. 2*A* illustrates spike-triggered average (STA) frames for two representative LGN neurons (*Left*: ON neuron in *Top* two rows; OFF neuron in *Bottom* two rows; stars

mark STA frames with peak pixel brightness) and temporal STA curves illustrating changes in peak pixel brightness across frames (*Right*). For these representative LGN neurons, both the temporal STA peak time (arrowheads in Fig. 2*A*, *Right*) and the full width at half height of the temporal STA were reduced with LED stimulation of CG feedback. Similar reductions in peak STA time and full width at half height of the temporal STA were observed across the sample of LGN neurons (Fig. 2 *B* and *C* and Table 1). The dramatic reductions in peak STA time and full width at half height of the temporal STA with LED stimulation of CG feedback suggest that enhanced CG feedback reduced stimulus-evoked response latencies among LGN neurons. These findings predict that LED stimulation of CG feedback should also reduce onset response latencies and variance of LGN neurons when stimulated with additional visual stimuli such as gratings.

We directly tested this prediction by examining the onset response latencies and spike-timing precision of LGN neuronal responses to repeated presentations of phase-reversing sinusoidal gratings with and without LED stimulation of CG feedback in six experimental animals. LED stimulation paired with grating presentation consisted of LED flashes synchronized to the start of each grating cycle (corresponding to every-other phase reversal). As illustrated for a single representative LGN neuron, LED stimulation of CG feedback sharpened the timing of LGN responses to each presentation of the preferred visual stimulus phase (Fig. 3 *A* and *B*). Supporting our prediction, LED stimulation of CG feedback led to a significant reduction in the onset response latencies of both LGN X and Y neurons (Fig. 3*C* and Table 2; refer to *Materials and Methods* for LGN neuronal type definitions). Furthermore, LED stimulation of CG feedback significantly increased spike-timing precision for both LGN X and Y neurons (Fig. 3*D* and Table 2). Thus, results of both m-sequence and sinusoidal grating tests independently support the notion that enhancing CG feedback significantly sharpens the temporal precision of LGN responses to visual inputs by reducing the time to the initial spike, prioritizing the shortest latency spikes, and eliminating lagging spikes. Additionally, the observed reductions in LGN response latencies with LED stimulation of CG feedback could not be explained by contrast-dependent phase advance or temporal phase advance mechanisms, nor were LED effects mediated by changes in brain state (*SI Appendix, Results* and Fig. S4).

To test the feedforward impact of CG-mediated sharpening of LGN temporal precision, we examined onset response latencies and spike-timing precision of neurons in the granular layers of V1 in three experimental animals. The granular layers include layer 4, which contains neurons that receive direct feedforward LGN input (5). We observed a nonsignificant ($P = 0.2$) reduction in onset response latencies among granular layer V1 neurons with LED stimulation of CG feedback (Fig. 3*E*). However, we observed a significant increase in spike-timing precision among V1 granular layer neurons with LED stimulation of CG feedback ($P = 0.01$; Fig. 3*F*). Large variations in onset response latencies among granular V1 neurons could be due to inclusion of multiple different neuronal types, including neurons not receiving direct LGN input, because onset response latencies among V1 neurons are dependent upon neuronal position within the cortical circuit hierarchy. Although spike-timing precision may

Table 1. STA metrics

Metric	All w/o LED, ms	All w/LED, ms	P value
STA peak time ($n = 15$)	66.3 ± 5.2	24.5 ± 5.6	0.0001
STA FWHH ($n = 15$)	69.0 ± 8.3	37.6 ± 5.2	0.01

M-sequence data from 6 of 11 experimental animals. FWHH, full width at half height; w/, with; w/o, without.
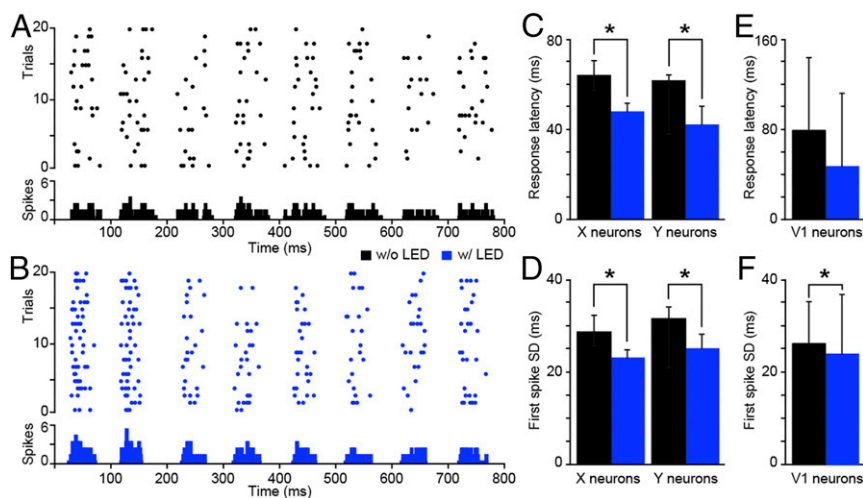
Fig. 3. LED stimulation of CG feedback reduces onset response latency and increases spike-timing precision. (*A* and *B*) Spike rasters and PSTHs of an example LGN Y neuron in response to 20 repeats of a phase-reversing grating without (*A*) and with (*B*) LED stimulation. PSTH bin width is 5 ms. (*C*) Average response latencies for LGN X ($n = 24$) and Y ($n = 20$) neurons without (black) and with (blue) LED stimulation. Error bars represent SEMs; asterisks indicate statistically significant differences for X and Y neurons separately at $P < 0.03$. (*D*) Average SD in first spike time per event for LGN X ($n = 12$) and Y ($n = 11$) neurons without (black) and with (blue) LED stimulation. Error bars represent SEMs; asterisks indicate statistically significant differences for X and Y neurons separately at $P < 0.05$. (*E*) Average response latency for V1 granular layer neurons ($n = 8$) without (black) and with (blue) LED stimulation. Error bars represent SEMs. Average V1 latency without LED is 79.3 ± 64.3; average V1 latency with LED is 47.1 ± 65.0. (*F*) Average SD in first spike time per event for V1 granular layer neurons ($n = 10$) without (black) and with (blue) LED stimulation. Error bars represent SEMs; the asterisk indicates a statistically significant difference ($P = 0.01$). Average SD of first spike time without LED is 54.2 ± 18.4; average SD of first spike time with LED is 49.5 ± 26.2.

also vary across V1 neuronal types, the observed increase in precision with LED stimulation of CG feedback likely arose via feedforward propagation from LGN to V1 as well as propagation among V1 circuits. These results demonstrate that enhanced CG feedback sharpens the temporal precision of LGN responses to more effectively transmit feedforward signals to V1.

Model Simulation of CG-Mediated Reduction in LGN Onset Response Latency. The average firing rate of putative CG neurons was 11.6% ($\pm 10.95\%$; $n = 6$ LEDR neurons from three experimental animals) greater when drifting gratings were paired with LED stimulation compared with presentation of gratings alone. To explore whether a modest increase in CG firing rate is sufficient to reduce LGN onset response latencies, we performed a model

simulation of LGN responses with and without LED stimulation of CG feedback (*Materials and Methods*). In our simplified simulation, the response of an LGN relay neuron was modeled as a weighted sum of retinal, inhibitory, and CG inputs (Fig. 4*A*). We obtained weights and the inhibitory disynaptic delay time by fitting the model to average LGN peristimulus-time histograms (PSTHs) recorded with and without LED stimulation of CG feedback (Fig. 4*B*, blue and black curves, respectively). A small increase in the weight of CG input (~6% increase) was sufficient to shift LGN onset response latency without altering the weights of the other inputs or the inhibitory disynaptic delay time (10 ms). A 6% increase in CG input weight is qualitatively consistent with the observed 11.6% increase in CG firing rate with LED stimulation (Fig. 4*C*). Thus, our simplified model provides theoretical evidence

Table 2. Response metrics

Metric	X, w/o LED	X, w/LED	Y, w/o LED	Y, w/LED	P value*
Onset response latency ($n = 44$; 24 X, 20 Y)	66.1 ± 8.0 ms	47.9 ± 4.8 ms	61.5 ± 7.6 ms	44.4 ± 6.6 ms	0.0006
First spike time SD ($n = 23$; 12 X, 11 Y)	27.3 ± 7.9 ms	24.3 ± 7.0 ms	31.6 ± 0.9 ms	25.2 ± 2.5 ms	0.002
c50 ($n = 49$; 26 X, 23 Y)	$56.2 \pm 2.7\%$	$57.1 \pm 4.2\%$	$34.2 \pm 3.3\%$	$33.6 \pm 3.6\%$	0.8
Preferred SF ($n = 33$; 18 X, 15 Y)	0.22 ± 0.03 cycle/°	0.23 ± 0.03 cycle/°	0.21 ± 0.02 cycle/°	0.20 ± 0.01 cycle/°	0.3
Preferred TF ($n = 37$; 19 X, 18 Y)	6.7 ± 0.7 Hz	7.4 ± 0.7 Hz	14.3 ± 2.2 Hz	14.0 ± 1.9 Hz	0.3
TF max firing rate ($n = 37$; 19 X, 18 Y)	13.7 ± 0.5 spikes/s	14.7 ± 0.5 spikes/s	14.1 ± 0.5 spikes/s	16.6 ± 0.8 spikes/s	0.04
TF norm. max. firing rate ($n = 37$; 19 X, 18 Y)	0.95 ± 0.01 spikes/s	1.0 ± 0.08 spikes/s	0.98 ± 0.01 spikes/s	1.28 ± 0.13 spikes/s	0.04
TF magnitude ($n = 37$; 19 X, 18 Y)	12.0 ± 1.2	14.5 ± 1.6	15.9 ± 1.5	22.6 ± 2.9	0.02

LGN physiology data from 6 of 11 experimental animals. max, maximum; norm, normalized; SF, spatial frequency; TF, temporal frequency; w/, with; w/o, without.

*Statistical comparisons are of all recorded LGN neurons (X and Y) across LED conditions because the sampled LGN subpopulations showed similar effects. Refer to figure legends for statistics for within-subpopulation comparisons (X alone, Y alone) across LED conditions.
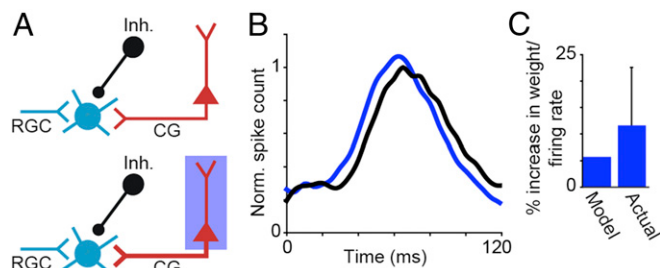
Fig. 4. Model simulation of CG impact on LGN onset response latency. (*A*) Schematics of model inputs to LGN relay neuron: retinal (RGC; cyan), CG (red), and inhibitory (Inh.; black). (*A*, *Upper*) Schematic illustration of visual stimulation alone. (*A*, *Bottom*) Schematic illustration of visual plus LED stimulation (the thicker CG axon indicates increased CG weight with LED stimulation; blue box). (*B*) Average LGN PSTHs in response to grating stimuli with (blue) and without (black) LED stimulation of CG feedback. (*C*) Histogram of model and actual increases in CG weight/firing rate with LED stimulation. Error bar represents SEM. Norm, normalized.

that small increases in CG neuronal firing rate can reduce the visual onset response latencies of LGN relay neurons and supports the notion that CG influence could be mediated through combination of monosynaptic excitation and disynaptic inhibition within the thalamus (Fig. 1*A*).

Influence of CG Feedback on LGN Neuronal Receptive Field Size and Tuning. Receptive fields and tuning properties of LGN neurons are mainly inherited from the retina and not from CG feedback. However, some prior studies of CG function have argued that feedback could modulate certain properties such as receptive field size (15). We found that LED stimulation of CG feedback significantly reduced the width of the classical receptive field for LGN neurons of both ON and OFF types (Fig. 2 *D* and *E* and Table 3). Although the effects of LED stimulation of CG feedback on LGN neuronal receptive field size varied across neurons (Fig. 2*D*), there were no relationships between CG influence on receptive field size and other neuronal characteristics such as X, Y, ON, or OFF type; preferred contrast, spatial, or temporal frequency; or retinotopic overlap with recorded LEDR neurons ($P > 0.5$ for all comparisons). In addition to reducing the width of the aggregate LGN classical receptive field, LED stimulation of CG feedback broadened the amplitude range within the receptive field (Fig. 2*E*), suggesting that CG feedback may have altered the contributions of classical and extraclassical receptive field subunits to spatial summation within the receptive field (32). Overall, the effect of LED stimulation of CG feedback was to narrow the spatial resolution of LGN receptive fields.

In six experimental animals, we measured LGN neuronal responses to drifting sinusoidal gratings with and without LED stimulation of CG feedback. Gratings were presented at the preferred temporal and spatial frequencies of the majority of simultaneously recorded LGN neurons, and LED flashes were synchronized to the start of each grating cycle. X and Y neuronal responses to gratings varying in contrast, spatial, and temporal frequency revealed no apparent changes in tuning curve shape with LED stimulation of CG feedback (Fig. 5 *A* and *B* and *SI Appendix*, Fig. S5 *A* and *B*). Specifically, response metrics—c50 (contrast to evoke half-maximal response), preferred spatial frequency, and preferred temporal frequency—were not altered with LED stimulation (Fig. 5*C* and Table 2). Interestingly, both the maximum firing rate (at the preferred temporal frequency) and the magnitude of the temporal frequency response were significantly increased for Y LGN neurons (Fig. 5*D*; maximum firing rate and magnitude were significantly increased with LED stimulation for the whole sample of LGN neurons, but not for X LGN neurons alone; Table 2). It is possible that the increase in maximum firing rate and response magnitude

observed for temporal frequency tuning tests was due to higher LED flash rates during temporal frequency tuning tests. During contrast and spatial frequency tuning tests, LED flashes were fixed at ~4 Hz, in synch with the fixed temporal frequency of those gratings. During temporal frequency tuning tests, the LED flashed at progressively increasing temporal frequencies, again in synch with the increasing temporal frequencies of the gratings. We performed two analyses to explore the discrepancies in LED modulation of LGN neurons across tuning tests: (*i*) comparison of predicted and actual grating plus LED modulation of LGN neurons; and (*ii*) examination of LGN responses when visual and LED stimulation was decoupled. Errors between predicted and actual tuning curves were equivalent across tuning tests, and results of visual/LED stimulus decoupling experiments also suggested that discrepancies in LED modulation of LGN neurons across tuning tests were explained by higher LED flash rates during temporal frequency tuning tests (*SI Appendix, Results*).

Given the marked change in receptive field shape with LED stimulation of CG feedback, it is somewhat puzzling that no obvious changes in spatial frequency tuning were observed. This discrepancy could be due in part to approximately three times greater pixel resolution for white noise compared with grating stimuli. However, a more parsimonious explanation may be related to the fact that LED stimulation of CG feedback increased the amplitude range within the receptive field (Fig. 2*E*). Spatial frequency curves are influenced by stimulus contrast and differential receptive field subunit contributions leading to changes in spatial summation within the receptive field (32). An increase in the amplitude range (or envelop) of the receptive field (as observed in Fig. 2*E*) is predicted to cause a narrowing of the spatial frequency tuning curve, especially for higher spatial frequencies, without altering the preferred spatial frequency (32). We observed just such a narrowing of LGN spatial frequency tuning curves with LED stimulation of CG feedback (*SI Appendix*, Fig. S5*C*). Thus, changes in receptive field shape were evident in both the white noise and grating data and together suggest that increased spatial resolution with LED stimulation of CG feedback was due to an increase in the amplitude range within the receptive field.

Finally, we examined whether LED stimulation of CG feedback altered the firing mode among LGN neurons. First, we determined that the vast majority of LGN neurons in our dataset (all but four) had spike waveforms matching regular spiking neurons (*SI Appendix*, Fig. S2*D*) based on peak-to-trough time and amplitude, suggesting that we recorded mainly from LGN relay neurons (8). We observed a low incidence of thalamic bursts (5) among recorded LGN neurons (<1% of spikes). A comparison of the percentage of burst spikes with and without LED stimulation of CG feedback yielded no significant change in burst firing for LGN neurons in our sample ($P > 0.9$).

Discussion

Characterizing the functional role of CG feedback in visual perception has remained a particularly stubborn puzzle in visual neuroscience. We took advantage of recent technological developments to selectively and reversibly manipulate the activity of CG neurons in a visual mammal, the ferret. Focal injections of

Table 3. Receptive field shape

Neuron type	w/o LED, °	w/o LED, °	P value*
ON (*n* = 7)	2.51 ± 0.4	1.25 ± 0.4	0.01
OFF (*n* = 8)	2.14 ± 0.6	1.15 ± 0.3	

M-sequence data from 6 of 11 experimental animals. RF, receptive field; w/, with; w/o, without.
*Statistical comparisons are of all recorded LGN neurons (ON and OFF) across LED conditions because the sampled LGN subpopulations showed similar effects.
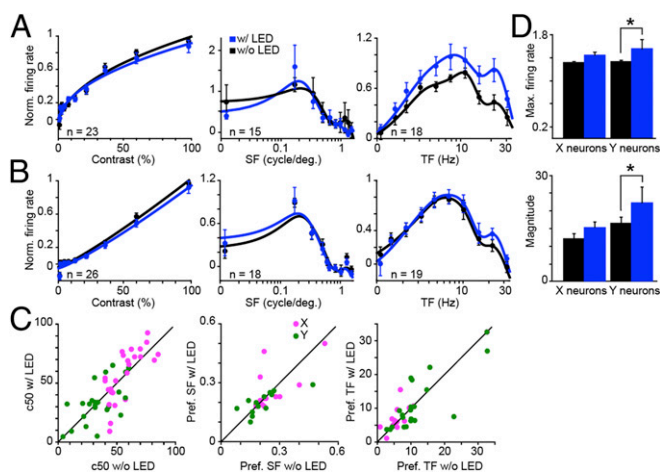
Fig. 5. LED stimulation of CG feedback does not alter LGN tuning preferences. (*A*) Population average contrast, spatial frequency (SF), and temporal frequency (TF) response curve fits for LGN Y neurons with (blue) and without (black) LED stimulation. Error bars represent SEMs. For each neuron and response curve, data (dots) are normalized to the peak of the without-LED response. (*B*) Population average response curve fits for LGN X neurons; conventions are as in *A*. (*C*) Scatterplots illustrate response metrics (c50 and preferred SF and TF) for LGN X (magenta) and Y (green) neurons with and without LED stimulation. (*D*) Average normalized maximum firing rate and magnitude for LGN X (*n* = 19) and Y (*n* = 18) neuronal responses to temporal frequency modulation without (black) and with (blue) LED stimulation. Error bars represent SEMs; asterisks indicate that LGN Y neurons alone demonstrate statistically significant differences (maximum firing rate, *P* = 0.04; magnitude, *P* = 0.049). Max, maximum; Norm, normalized; Pref, preferred; w/, with; w/o, without.

rabies virus expressing ChR2 and mCherry into the LGN resulted in gene expression in CG neurons in layer 6 of the visual cortex such that CG neurons were driven by LED stimulation (Fig. 1). We demonstrate that stimulation of CG feedback causes a reduction in the stimulus-to-response latency, independently measured with drifting grating and white noise stimuli, as well as an increase in the spike-timing precision of LGN neurons (Figs. 2 and 3). Furthermore, enhancing CG feedback also increased the response precision of neurons in the granular layers of V1 (Fig. 3*F*). We modeled a simple circuit mechanism by which CG feedback could influence LGN temporal precision and discovered that a small increase in CG input is sufficient to shift the response latency of LGN relay neurons (Fig. 4). Consistent with the notion that LGN tuning preferences are mainly inherited from retinal inputs, LED stimulation of CG feedback did not alter LGN neuronal tuning preferences (Fig. 5). However, we observed a significant reduction in the size of the classical receptive field of LGN neurons with enhancement of CG feedback (Fig. 2 *D* and *E*). Together, these findings demonstrate that CG feedback dramatically sharpens the precision of LGN neuronal responses to visual inputs by privileging the shortest latency spikes, eliminating sluggish responses, and shrinking the size of the classical receptive field. Furthermore, because increased temporal precision among LGN relay neurons is fed forward to V1, CG feedback increases the overall precision of feedforward signal transmission.

We demonstrate that CG feedback reduces the latency of LGN responses and increases the spike-timing precision of both LGN and granular layer V1 neuronal responses. We observed two significant reductions in LGN response variance with enhanced CG feedback: (*i*) prioritization of the shortest-latency spikes in response to incoming visual inputs, quantified as a reduction in the SD of the first spike time; and (*ii*) elimination of sluggish spikes, evident as a significant reduction in the full width

at half height of the temporal STA. These reductions in LGN response variance are consistent with the predictions of Andolina and colleagues (16), who found significant decreases in stimulus modulation and increases in response variability among LGN neurons when the cortex of anesthetized cats was inactivated with muscimol. Also consistent is the finding that selective destruction of CG neurons led to a broadening of the interspike-interval distribution of tonic spikes recorded during synchronized EEG states (17).

In parallel with our discovery that enhanced CG feedback increases the temporal precision of LGN responses, we also observed changes in LGN receptive field shape, including a reduction in the size of the classical receptive field and an increase in the amplitude range within the receptive field. The observed reduction in classical receptive field size with enhanced CG feedback is consistent with the finding that pharmacological inactivation of cat visual cortex led to an increase in the size of LGN receptive fields (15). These authors also demonstrated that the strength of surround suppression was reduced when CG feedback was inactivated (15). It is therefore possible that enhanced CG feedback increases the influence of the surround, leading to a reduction in the effective size of the classical receptive field. We observed narrowing and elongation of the aggregate LGN spatial receptive field and a reduction in the width of LGN spatial frequency tuning curves, consistent with the idea that enhancing CG feedback alters receptive field subunit contributions (32). The notion that CG feedback sharpens the spatial resolution of LGN responses is further supported by computational models of LGN–V1–TRN circuits in which stimulation of retinotopically aligned V1/LGN neurons led to enhanced activity in LGN relay neurons with aligned receptive fields and suppressed activity in neighboring relay neurons (33). Interestingly, CG feedback in the mouse visual system does not appear to modulate the size of the classical receptive field or the influence of the surround among LGN neurons (8). Although species differences could explain these contradictory findings, the prediction that CG feedback enhances surround suppression in a highly visual mammal remains to be tested using selective methods.

It has long been suggested that the corticothalamic feedback implements gain control in the thalamus (34). Indeed, numerous studies using a variety of experimental techniques to manipulate CG feedback have documented changes in the magnitude of LGN responses (7–14). Our results are consistent with some, but not all, of these observations. Specifically, our finding that enhanced CG feedback increases the magnitude of LGN responses to grating stimuli varying in temporal frequency is consistent with prior observations in anesthetized cats and primates of decreased LGN responses to moving bar or drifting grating stimuli without changes in tuning preferences when the cortex was either aspirated or cooled (9, 11). In studies focusing on CG feedback and contrast sensitivity, cooling V1 in anesthetized monkeys led to a reduction in the gain of contrast response functions for parvocellular LGN neurons (13), and ablating V1 in anesthetized cats resulted in decreased contrast adaptation that was more pronounced in LGN Y neurons compared with X neurons (10). In the mouse, optogenetic suppression of CG feedback resulted in a variety of contrast response magnitude changes in the LGN, including increases, decreases, and no change in contrast response magnitude (8). We did not observe systematic increases or decreases in contrast response magnitude in LGN X or Y neurons (similarly, we did not observe systematic magnitude modulation of spatial frequency responses), more consistent with the findings in the mouse visual system. Notably, some of the previously observed contrast gain changes were specific to particular LGN cell types, for example parvocellular neurons in monkey LGN (13) and Y neurons in cat LGN (10). We also observed larger increases in the magnitude of temporal frequency responses for LGN Y neurons compared with X neurons.

Together, these findings support the notion that CG feedback may affect LGN neurons in a stream-specific fashion (35).

We propose and simulate a simple circuit mechanism, based on the known anatomy of CG circuits, by which CG feedback sharpens both the temporal and spatial resolution of LGN neuronal responses (5). CG axons synapse onto LGN relay neurons, LGN interneurons, and TRN neurons (3–5) (Fig. 1A), forming "modulatory" glutamatergic synapses that are facilitating, in contrast to retinogeniculate "driving" synapses onto LGN relay neurons and interneurons that are depressing (36–38). Thus, CG feedback can both depolarize and hyperpolarize LGN relay neurons via direct monosynaptic excitation and indirect disynaptic inhibition, respectively. Through these excitatory and inhibitory connections, CG feedback could reduce LGN response latency and enhance response precision by (i) privileging the shortest-latency spikes in LGN relay neurons through monosynaptic depolarization, and (ii) eliminating sluggish spikes in LGN relay neurons through delayed hyperpolarization via disynaptic GABAergic inputs from LGN interneurons and TRN neurons (39–41), both of which receive glutamatergic CG input (12, 42). Our model simulation supports this simple circuit mechanism and further suggests that a small increase in the weight of CG input is sufficient to reduce response latencies among LGN relay neurons (Fig. 4). Our model simulation does not rule out additional mechanisms by which enhanced CG feedback could alter LGN responses. For example, CG feedback could alter the baseline conductance or conductance noise of postsynaptic LGN neurons, causing a change in the membrane time constant and leading to a more reliable input/output transfer function (43). Changes in LGN response latencies could also result from global modulations of brain state or shifts in LGN spiking mode; however, we did not observe changes in EEG state (*SI Appendix*, Fig. S4) or burst spiking across conditions with and without LED stimulation of CG feedback, consistent with observations in the mouse visual system (8) (but see ref. 12).

The CG pathway is the first feedback circuit in the visual hierarchy. It is interesting to consider how CG neurons are initially activated to influence LGN temporal dynamics. Some CG neurons receive driving, monosynaptic input directly from the LGN (44), and all CG neurons likely receive strong input from geniculocortical-recipient neurons in layer 4 (45, 46). Because these subcortical and local inputs are stream-specific (44, 45), CG neurons receive selective information about particular features of the visual world, as evidenced by their stream-specific physiological response properties (35). Thus, particular features of a visual scene could trigger CG activation, causing stream-specific feedback activation of LGN ensembles via the circuit mechanism described above. Interestingly, CG feedback in a variety of species is known to operate on different timescales due to differential axon conduction velocities among the diverse CG neuronal types (35, 44, 47–51). The large variation in axon conduction times suggests that different CG neurons may have shorter or longer timescales over which they can integrate incoming information. We observed similar effects on LGN response precision when CG neurons were intermittently optogenetically stimulated and when optogenetic stimulation was sustained, suggesting that the mechanism by which CG feedback alters LGN temporal precision may be consistent across CG activation timescales.

A strength of our study is our selective manipulation of CG neurons in a highly visual mammal. It is important to note that optogenetic stimulation, even when it is restricted to a single neuronal population located within a single cortical hypercolumn, probably does not mimic natural visual stimulation. How might our results differ if our experiment had been performed under more naturalistic conditions? There are a number of neuronal properties that should remain invariant to natural/unnatural stimulation and/or brain state. For example, axon condition latencies, visual response

latencies, and visual response properties are for the most part invariant, whereas neuronal firing rates are reduced with anesthesia (44, 52, 53). Our findings that are more dependent upon invariant properties, such as axon conduction latency, should hold up across a variety of conditions. Accordingly, the reduction in LGN response latency with enhanced CG feedback may remain consistent across visual stimulus conditions and arousal states. However, it is possible that other observations, such as the reduction in receptive field size and the reduction in response variance, may be more susceptible to natural versus unnatural visual stimulation conditions and changes in attention or arousal state. Optogenetic stimulation, like electrical stimulation, probably leads to increased synchronization of neuronal responses compared with natural visual stimulation. Given that CG axons conduct at different speeds, it is not clear how synchronized CG stimulation might impact LGN responses. Indeed, future studies using selective techniques to modulate CG activity in a naturalistic manner in alert, behaving, and highly visual mammals will be required to address these important questions.

Prior theoretical (39–41, 54) and experimental evidence (16) supports the hypothesis that CG feedback alters the timing of LGN responses. Here, we demonstrate concretely that CG feedback reduces the latency and variability of visually evoked responses, enhances the spike-timing precision of those responses, and sharpens the spatial receptive field. Sharpened temporal precision could lead to synchronization of activity among ensembles of LGN neurons (55) to increase the efficacy of feedforward information transmission from LGN to V1. In support of this hypothesis, we observed an increase in the precision of visually evoked responses among V1 neurons with LED stimulation of CG feedback. Overall, our results support the notion that the thalamus is much more than a simple sensory relay station. Corticothalamic circuits exert powerful influence over thalamic processing by controlling the timing and precision of sensory signals traveling from peripheral receptors to the sensory cortex. Thus, whereas feedforward sensory circuits convey information about features of the sensory environment, cortical feedback circuits are responsible for refining those signals.

Materials and Methods

Twenty adult female ferrets (*Mustela putorius furo*) were used in this study. All animal procedures were approved by the Institutional Animal Care and Use Committee at Dartmouth and conformed to the guidelines for animal use set forth by the US Department of Agriculture and NIH. To express the optogenetic cation channel channelrhodopsin2 and the fluorescent marker mCherry selectively in corticogeniculate neurons in the visual cortex, a genetically modified rabies virus (SADΔG-ChR2-mCherry) was injected into the lateral geniculate nucleus, where it was taken up by axon terminals at the injection site, including axons of CG neurons. G-deleted rabies virus cannot move transsynaptically, as wild-type rabies would, because the essential glycoprotein is not endogenously expressed (22). Thus, G-deleted rabies virus acts like a retrograde tracer, traveling along axons to infect cell bodies. Rabies virus replicates within infected neurons, resulting in robust expression of proteins translated from viral genes including inserted genes of interest, in this case ChR2 and mCherry (21). Injection of SADΔG-ChR2-mCherry into the LGN caused expression of ChR2 and mCherry in retinogeniculate neurons, thalamic reticular nucleus neurons, LGN interneurons, and CG neurons, because these populations have axon terminals in the LGN. Importantly, because CG neurons are the only visual cortical neurons with axon terminals in the LGN (26–28), they are the only neurons in the cortex expressing ChR2 and mCherry following injection of virus into the LGN (Fig. 1C and *SI Appendix*, Fig. S1 C and D). Furthermore, injection of SADΔG-ChR2-mCherry into the white matter, hippocampus, ventricle, and somatosensory cortex did not result in any labeled neurons in the visual cortex (*n* = 9 animals), indicating that virus was not taken up by axons of passage. Of the 11 experimental animals included in this study, 2 animals were used for histology only, 6 animals were used to collect LGN physiology data (in 4 of these animals, V1 physiology data were also collected), and 3 animals were used to collect additional m-sequence data from LGN neurons. Of the 9 control animals, all were used for histology and physiological recordings in LGN, and 3 were used for physiological recordings in V1.

For a detailed description of the experimental methods, please refer to *SI Appendix, Materials and Methods*. Experimental methods are briefly summarized here. G-deleted rabies virus was surgically injected into the LGN of

ferrets in sterile surgery using aseptic techniques. Location and depth of the LGN were determined neurophysiologically, and 5 μL SADΔG-ChR2-mCherry was injected through glass pipettes at the identified LGN location. Animals recovered for 7 to 11 d to allow for adequate expression of optogenetic proteins in infected CG neurons (21, 22). Neurophysiological recordings were conducted in anesthetized and paralyzed animals 7 to 11 d following sur-gical injection of virus. Subcranial EEG was recorded to monitor anesthetic depth and brain state. All visual stimuli were designed with custom-written Matlab (MathWorks) command scripts, generated with a ViSaGe stimulus generation system (Cambridge Research Systems), and presented on a CRT monitor (ViewSonic) placed 45 to 60 cm in front of the animals' eyes. Visual stimuli included grayscale drifting sinusoidal gratings, phase-reversing gratings, and white noise m-sequence stimuli. Grating stimuli were pre-sented for 2 s followed by 2 s of mean gray. Gratings were between 8 and 20° in diameter such that a single grating overlapped all simultaneously recorded neurons. When not varying, grating parameters were fixed at the preferred spatial and temporal frequencies of the majority of recorded LGN neurons, preferred orientation of recorded V1 neurons, and a contrast of 70%. All grating stimuli were displayed four times, twice with LED stimu-lation and twice without LED stimulation of CG feedback. M-sequence stimuli were 8 to 25° on each side of a square 24 × 24-pixel grid and were displayed for 10 to 20 min on each of two repeats, once with and once without LED stimulation of CG feedback. A blue LED was positioned over V1 with the cannula embedded in the agar overlying the cortex. Estimated LED power in layer 6 was a maximum of 1 mW/mm², and relative spatial spread of the LED corresponded to approximately one functional hypercolumn in V1 (*SI Appendix*, Fig. S2F). The LED was flashed at the same temporal fre-quency as drifting gratings and was on continuously during m-sequence presentation. Neuronal responses to LED-only stimulation were quantified by recording neuronal responses to LED flashes varying in flash frequency between 1 and 16 Hz.

Extracellular spikes and local field potentials were recorded from two multielectrode arrays inserted into the LGN (7-channel Eckhorn Matrix; Thomas Recording) and in V1 (24-contact U-Probe; Plexon). Recordings of LGN neurons, putative CG neurons (LED-responsive or LEDR), and other V1 neurons (non-LEDR) were recorded in experimental and control animals in response to presentations of visual stimuli alone or visual stimuli paired with LED stimulation. LGN X and Y neurons were classified based on their responses to drifting gratings

varying in contrast and temporal frequency. X neurons prefer higher-contrast stimuli and lower temporal frequencies (56), so we defined X neurons as those with contrast-to-evoke-half-maximal-response values ≥40% and higher-temporal-frequency-to-evoke-half-maximal-response (TFhigh50) values on the order of ≤15 Hz. Y neurons respond to lower-contrast stimuli and follow higher temporal frequencies, so we defined Y neurons as those with c50 values <40% and TFhigh50 values greater than 15 Hz (average X TFhigh50, 15.5 ± 1.2 Hz; average Y TFhigh50, 20.4 ± 1.9 Hz). Quantifications of neuronal responses in-cluded spontaneous firing rate, average stimulus evoked firing rate per trial, maximum firing rate in response to preferred stimuli, average stimulus-evoked onset response latency as the time to reach 50% of the maximum firing rate following stimulus onset, magnitude of response as the integral of normalized tuning curves, and percentage of burst spikes among LGN neurons. Spike-triggered averages of frames preceding LGN spikes were measured for LGN neurons. From these STAs, classical receptive field widths as well as temporal modulations in peak pixel luminance were calculated. Spike-timing precision was quantified from LGN and V1 peristimulus-time histograms as the SD of the first spike time in each event (57).

LGN responses were modeled as a weighted sum of retinal, CG, and inhibitory inputs according to the following equation: $X_{LGN}(t) = W_{RGC} \times X_{RGC}(t) + W_{CG} \times X_{CG}(t) + W_{Inh} \times X_{Inh}(t + tau)$, where $X(t)$s are PSTHs, Ws represent weights, and tau is the disynaptic inhibition delay time. Latencies and time courses for retinal and inhibitory PSTHs were adapted from the literature (58–60), and the CG PSTH was the average LEDR PSTH measured without LED stimulation.

Following neurophysiological recording sessions, animals were euthanized and perfused such that brain tissue could be removed and processed histo-logically. Antibody staining against mCherry was performed to permanently stain all virus-infected neurons.

1. Jones EG (2002) Thalamic organization and function after Cajal. *Prog Brain Res* 136: 333–357.
2. Briggs F, Usrey WM (2011) Corticogeniculate feedback and parallel processing in the primate visual system. *J Physiol* 589:33–40.
3. Claps A, Casagrande VA (1990) The distribution and morphology of corticogeniculate axons in ferrets. *Brain Res* 530:126–129.
4. Eriṣir A, Van Horn SC, Sherman SM (1997) Relative numbers of cortical and brainstem inputs to the lateral geniculate nucleus. *Proc Natl Acad Sci USA* 94:1517–1520.
5. Sherman SM, Guillery RW (2006) *Exploring the Thalamus and Its Role in Cortical Function* (MIT Press, Boston), 2nd Ed.
6. Usrey WM, Reppas J, Reid RC (1998) Paired-spike interactions and synaptic efficacy of retinal inputs to the thalamus. *Nature* 395:384–387.
7. Cudeiro J, Rivadulla C, Grieve KL (2000) Visual response augmentation in cat (and macaque) LGN: Potentiation by corticofugally mediated gain control in the temporal domain. *Eur J Neurosci* 12:1135–1144.
8. Denman DJ, Contreras D (2015) Complex effects on in vivo visual responses by specific projections from mouse cortical layer 6 to dorsal lateral geniculate nucleus. *J Neurosci* 35:9265–9280.
9. Gulyás B, Lagae L, Eysel UT, Orban GA (1990) Corticofugal feedback influences the responses of geniculate neurons to moving stimuli. *Exp Brain Res* 79:441–446.
10. Li G, Ye X, Song T, Yang Y, Zhou Y (2011) Contrast adaptation in cat lateral geniculate nucleus and influence of corticothalamic feedback. *Eur J Neurosci* 34:622–631.
11. Marrocco RT, McClurkin JW, Alkire MT (1996) The influence of the visual cortex on the spatiotemporal response properties of lateral geniculate nucleus cells. *Brain Res* 737: 110–118.
12. Olsen SR, Bortone DS, Adesnik H, Scanziani M (2012) Gain control by layer six in cortical circuits of vision. *Nature* 483:47–52.
13. Przybyszewski AW, Gaska JP, Foote W, Pollen DA (2000) Striate cortex increases contrast gain of macaque LGN neurons. *Vis Neurosci* 17:485–494.
14. Wörgötter F, Eyding D, Macklis JD, Funke K (2002) The influence of the cortico-thalamic projection on responses in the thalamus and cortex. *Philos Trans R Soc Lond B Biol Sci* 357:1823–1834.
15. Andolina IM, Jones HE, Sillito AM (2013) Effects of cortical feedback on the spatial properties of relay cells in the lateral geniculate nucleus. *J Neurophysiol* 109:889–899.
16. Andolina IM, Jones HE, Wang W, Sillito AM (2007) Corticothalamic feedback en-hances stimulus response precision in the visual system. *Proc Natl Acad Sci USA* 104: 1685–1690.
17. Eyding D, Macklis JD, Neubacher U, Funke K, Worgotter F (2003) Selective elimination of corticogeniculate feedback abolishes the electroencephalogram dependence of primary visual cortical receptive fields and reduces their spatial specificity. *J Neurosci* 23:7021–7033.
18. Crandall SR, Cruikshank SJ, Connors BW (2015) A corticothalamic switch: Controlling the thalamus with dynamic synapses. *Neuron* 86:768–782.
19. Jackson CA, Hickey TL (1985) Use of ferrets in studies of the visual system. *Lab Anim Sci* 35:211–215.
20. Airan RD, Thompson KR, Fenno LE, Bernstein H, Deisseroth K (2009) Temporally precise in vivo control of intracellular signalling. *Nature* 458:1025–1029.
21. Osakada F, et al. (2011) New rabies virus variants for monitoring and manipulating activity and gene expression in defined neural circuits. *Neuron* 71:617–631.
22. Wickersham IR, Finke S, Conzelmann KK, Callaway EM (2007) Retrograde neuronal tracing with a deletion-mutant rabies virus. *Nat Methods* 4:47–49.
23. Ghanem A, Conzelmann KK (2016) G gene-deficient single-round rabies viruses for neuronal circuit analysis. *Virus Res* 216:41–54.
24. Kelly RM, Strick PL (2000) Rabies as a transneuronal tracer of circuits in the central nervous system. *J Neurosci Methods* 103:63–71.
25. Ugolini G (2010) Advances in viral transneuronal tracing. *J Neurosci Methods* 194:2–20.
26. Fitzpatrick D, Usrey WM, Schofield BR, Einstein G (1994) The sublaminar organization of corticogeniculate neurons in layer 6 of macaque striate cortex. *Vis Neurosci* 11:307–315.
27. Hendrickson AE, Wilson JR, Ogren MP (1978) The neuroanatomical organization of pathways between the dorsal lateral geniculate nucleus and visual cortex in the Old World and New World primates. *J Comp Neurol* 182:123–136.
28. Lund JS, Lund RD, Hendrickson AE, Bunt AH, Fuchs AF (1975) The origin of efferent pathways from the primary visual cortex, area 17, of the macaque monkey as shown by retrograde transport of horseradish peroxidase. *J Comp Neurol* 164:287–303.
29. Briggs F, Kiley CW, Callaway EM, Usrey WM (2016) Morphological substrates for parallel streams of corticogeniculate feedback originating in both V1 and V2 of the macaque monkey. *Neuron* 90:388–399.
30. Katz LC (1987) Local circuitry of identified projection neurons in cat visual cortex brain slices. *J Neurosci* 7:1223–1249.
31. Gilbert CD, Kelly JP (1975) The projections of cells in different layers of the cat's visual cortex. *J Comp Neurol* 163:81–105.
32. Sceniak MP, Hawken MJ, Shapley R (2002) Contrast-dependent changes in spatial frequency tuning of macaque V1 neurons: Effects of a changing receptive field size. *J Neurophysiol* 88:1363–1373.
33. Bickle J, Bernstein M, Heatley M, Worley C, Stiehl S (1999) A functional hypothesis for LGN-V1-TRN connectivities suggested by computer simulation. *J Comp Neurosci* 6:251–261.

34. Briggs F, Usrey WM (2008) Emerging views of corticothalamic function. *Curr Opin Neurobiol* 18:403–407.

35. Briggs F, Usrey WM (2009) Parallel processing in the corticogeniculate pathway of the macaque monkey. *Neuron* 62:135–146.

36. Alexander GM, Godwin DW (2005) Presynaptic inhibition of corticothalamic feedback by metabotropic glutamate receptors. *J Neurophysiol* 94:163–175.

37. Jurgens CWD, Bell KA, McQuiston AR, Guido W (2012) Optogenetic stimulation of the corticothalamic pathway affects relay cells and GABAergic neurons differently in the mouse visual thalamus. *PLoS One* 7:e45717.

38. Sherman SM, Guillery RW (1998) On the actions that one nerve cell can have on another: Distinguishing "drivers" from "modulators." *Proc Natl Acad Sci USA* 95: 7121–7126.

39. Bal T, Debay D, Destexhe A (2000) Cortical feedback controls the frequency and synchrony of oscillations in the visual thalamus. *J Neurosci* 20:7478–7488.

40. Destexhe A (2000) Modelling corticothalamic feedback and the gating of the thalamus by the cerebral cortex. *J Physiol Paris* 94:391–410.

41. Funke K, Nelle E, Li B, Worgotter F (1996) Corticofugal feedback improves the timing of retino-geniculate signal transmission. *Neuroreport* 7:2130–2134.

42. Zhang L, Jones EG (2004) Corticothalamic inhibition in the thalamic reticular nucleus. *J Neurophysiol* 91:759–766.

43. Wolfart J, Debay D, Le Masson G, Destexhe A, Bal T (2005) Synaptic background activity controls spike transfer from thalamus to cortex. *Nat Neurosci* 8:1760–1767.

44. Briggs F, Usrey WM (2007) A fast, reciprocal pathway between the lateral geniculate nucleus and visual cortex in the macaque monkey. *J Neurosci* 27:5431–5436.

45. Briggs F, Callaway EM (2001) Layer-specific input to distinct cell types in layer 6 of monkey primary visual cortex. *J Neurosci* 21:3600–3608.

46. Douglas RJ, Martin KA (2004) Neuronal circuits of the neocortex. *Annu Rev Neurosci* 27:419–451.

47. Harvey AR (1978) Characteristics of corticothalamic neurons in area 17 of the cat. *Neurosci Lett* 7:177–181.

48. Tsumoto T, Creutzfeldt OD, Legendy CR (1978) Functional organization of the corticofugal system from visual cortex to lateral geniculate nucleus in the cat. *Exp Brain Res* 32:345–364.

49. Swadlow HA, Weyand TG (1987) Corticogeniculate neurons, corticotectal neurons, and suspected interneurons in visual cortex of awake rabbits: Receptive-field properties, axonal properties, and effects of EEG arousal. *J Neurophysiol* 57:977–1001.

50. Grieve KL, Sillito AM (1995) Differential properties of cells in the feline primary visual cortex providing the corticofugal feedback to the lateral geniculate nucleus and visual claustrum. *J Neurosci* 15:4868–4874.

51. Briggs F, Usrey WM (2005) Temporal properties of feedforward and feedback pathways between thalamus and visual cortex in the ferret. *Thalamus Relat Syst* 3:133–139.

52. Alitto HJ, Moore BD, Rathbun DL, Usrey WM (2011) A comparison of visual responses in the lateral geniculate nucleus of alert and anesthetized macaque monkeys. *J Physiol* 589:87–99.

53. Sellers KK, Bennett DV, Hutt A, Williams JH, Frohlich F (2015) Awake vs. anesthetized: Layer-specific sensory processing in visual cortex and functional connectivity between cortical areas. *J Neurophysiol* 113:3798–3815.

54. Yousif N, Denham M (2007) The role of cortical feedback in the generation of the temporal receptive field responses of lateral geniculate nucleus neurons: A computational modelling study. *Biol Cybern* 97:269–277.

55. Sillito AM, Jones HE, Gerstein GL, West DC (1994) Feature-linked synchronization of thalamic relay cell firing induced by feedback from the visual cortex. *Nature* 369:479–482.

56. Sherman SM, Spear PD (1982) Organization of visual pathways in normal and visually deprived cats. *Physiol Rev* 62:738–855.

57. Berry MJ, Warland DK, Meister M (1997) The structure and precision of retinal spike trains. *Proc Natl Acad Sci USA* 94:5411–5416.

58. McAlonan K, Cavanaugh JR, Wurtz RH (2008) Guarding the gateway to cortex with attention in visual thalamus. *Nature* 456:391–394.

59. Rathbun DL, Warland DK, Usrey WM (2010) Spike timing and information transmission at retinogeniculate synapses. *J Neurosci* 30:13558–13566.

60. Cafaro J, Rieke F (2013) Regulation of spatial selectivity by crossover inhibition. *J Neurosci* 33:6310–6320.